



Some Organotellurium(IV) Complexes of 1-Methyl-3-(*p*-tolylimino)indolin-2-one Schiff Base

MANISH KUMAR^{1D}, K.K. VERMA^{1D} and SAPANA GARG^{*1D}

Department of Chemistry, Maharishi Dayanand University, Rohtak-124001, India

*Corresponding author: E-mail: sapanagarg1511@gmail.com

Received: 8 February 2021;

Accepted: 22 March 2021;

Published online: 5 June 2021;

AJC-20349

Six new hexa-coordinated organotellurium(IV) complexes of type $R\text{TeCl}_3\cdot\text{NMeIPT}$ and $R_2\text{TeCl}_2\cdot\text{NMeIPT}$ ($R = 4\text{-hydroxyphenyl}$, 4-methoxyphenyl or $3\text{-methyl-4-hydroxyphenyl}$; $\text{NMeIPT(L)} = \text{Schiff base (1-methyl-3-(p-tolylimino)indolin-2-one)}$ derived from condensation of 4-methylisatin and *p*-toluidine) have been synthesized and characterized by different spectral studies like elemental analyses, molar conductance, infrared, mass spectrometry, $^1\text{H NMR}$, $^{13}\text{C NMR}$ and UV-visible spectroscopy. On the basis of spectroscopic data, it is evident that Schiff base behaves as NO donor bidentate ligand *via* azomethine nitrogen atom and oxygen atom from carbonyl group for all the tellurium(IV) complexes. The results showed that all the organotellurium(IV) complexes possess distorted octahedral geometry. Geometry of the all organotellurium(IV) complexes was optimized and their theoretical quantum mechanical parameters were calculated. This computational study also suggests octahedral geometry for complexes. The antimicrobial activity of NMeIPT and all the organotellurium(IV) complexes were screened against bacteria *i.e.* *Xanthomonas campestris* and *Bacillus cereus* and fungi *i.e.* *Fusarium oxysporum*, *Candida albicans* and *Sclerotinia sclerotium*.

Keywords: *N*-Methylisatin, *p*-Toluidine, Organotellurium complexes, Antibacterial activity, Antifungal activity.

INTRODUCTION

1*H*-Indole-2,3-dione (isatin) and its derivatives are important polyfunctional heterocyclic compounds and known to possess variety of biological activities. *N*-Alkylation of isatin reduces its lability towards bases, while maintaining its reactivity. The chemical versatility of these compounds led to their extensive use as intermediates, synthetic precursors for preparation of important heterocyclic compounds and raw material for drug synthesis. Schiff bases of isatin and its derivatives possess an extensive range of medicinal properties including tuberculosis [1,2], anti-HIV [3,4], antiviral [5,6], anticonvulsant [7], anti-helminthic [8], antibacterial [9], antifungal [10,11] and anti-inflammatory [12] activities.

Several organotellurium complexes *viz.* $R\text{TeCl}_3$ (organotellurium(IV) trichlorides) and $R_2\text{TeCl}_2$ (diorganotellurium(IV) dichlorides) are known to behave as electron acceptors and can form stable complexes [13-17] when react with several O, N and S atom donor ligands. In continuation of earlier work [18-20] of Schiff base ligands derived from isatin derivative with organotellurium(IV) chlorides, In this article, the studies of organotellurium(IV) complexes synthesized by reactions

of $R\text{TeCl}_3$ and $R_2\text{TeCl}_2$ with new Schiff base (NMeIPT) are presented. The structures of the synthesized tellurium(IV) complexes were determined by using different spectroscopic techniques. The Schiff base ligand and all the synthesized organotellurium (IV) complexes have been screened out for their antibacterial and antifungal activities.

EXPERIMENTAL

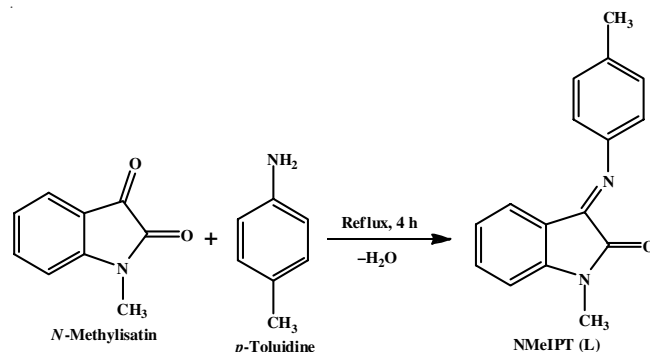
All the chemicals used were of analytical grade and procured from the reputed commercial sources. *N*-Methylisatin, *p*-toluidine, tellurium tetrachloride, anisole, phenol and *o*-cresol were supplied by Sigma-Aldrich. The standard procedures [21,22] were used to purify the organic solvents. The solvents were stored over molecular sieves. Organotellurium(IV) trichlorides and diorganotellurium (IV) dichlorides compounds were synthesized under the dry atmosphere of nitrogen.

Melting points of all the compounds were obtained by using open capillaries and are uncorrected. FT-IR spectra of NMeIPT and organotellurium(IV) complexes were recorded on FT-IR spectrophotometer (NICOLET iS50) in KBr pallets in the mid IR region and in Polyethylene in the far IR region. (ESI-MS) Mass spectra of Schiff base ligand and its organotellurium(IV)

complexes were recorded on Mass Analyzer. Molar conductance measurements of all complexes were made using conductivity cell with 10^{-3} M solutions in DMSO at 25 ± 1 °C. CHN analyses were carried out on a Thermo-Finnigan CHNS analyzer. The UV-Vis spectra were recorded on Shimadzu UV-3600 Plus, while ^1H & ^{13}C NMR were recorded with 400 NMR spectrometer (BRUKER AVANCE II) by using TMS as references in DMSO.

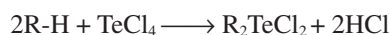
Synthesis of 1-methyl-3-(*p*-tolylimino)indolin-2-one (NMeIPT) ligand [23,24]: *N*-Methylisatin (0.02 mol, 3.22 g) was dissolved in 25 mL of ethanol. This solution was added to ethanolic solution of *p*-toluidine (0.02 mol, 2.14 g). After complete addition, the reaction mixture was refluxed for 4 h with continuous stirring on a water bath. A red coloured solid was collected, recrystallized from ethanol and dried in vacuum (**Scheme-I**). *m.w.*: 250.30 g/mol; *m.p.*: 134-137 °C, yield: 80.43% (4.10 g), colour: red. ^1H NMR (600 MHz, DMSO- d_6 , δ ppm): 7.63-6.59 (m, 8H, Ar-H), 3.21 (s, 3H, N-CH₃), 2.37 (s, 3H). ^{13}C NMR (600 MHz, DMSO- d_6 , δ ppm): 162.84 (C₉), 155.24 (C₂), 147.80 (C₁₁), 145.82 (C₈), 138.09 (C₆), 134.30 (C₁₃, C₁₅), 122.10 (C₁₅), 122.91 (C₅), 119.97 (C₄), 119.12 (C₃), 116.90 (C₁₄), 110.29 (C₇), 126.28 (C₁₂, C₁₆), 26.49 (C₁₀), 20.42 (C₁₇). Elemental analysis for ligand L (*m.f.* C₁₅H₁₂N₂O₂) calcd. (found) %: C, 76.78 (76.42); H, 5.64 (5.79); N, 11.19 (11.10).

Synthesis of RTeCl₃ (organotellurium(IV) trichlorides) and R₂TeCl₂ (diorganotellurium(IV) dichlorides): Electro-

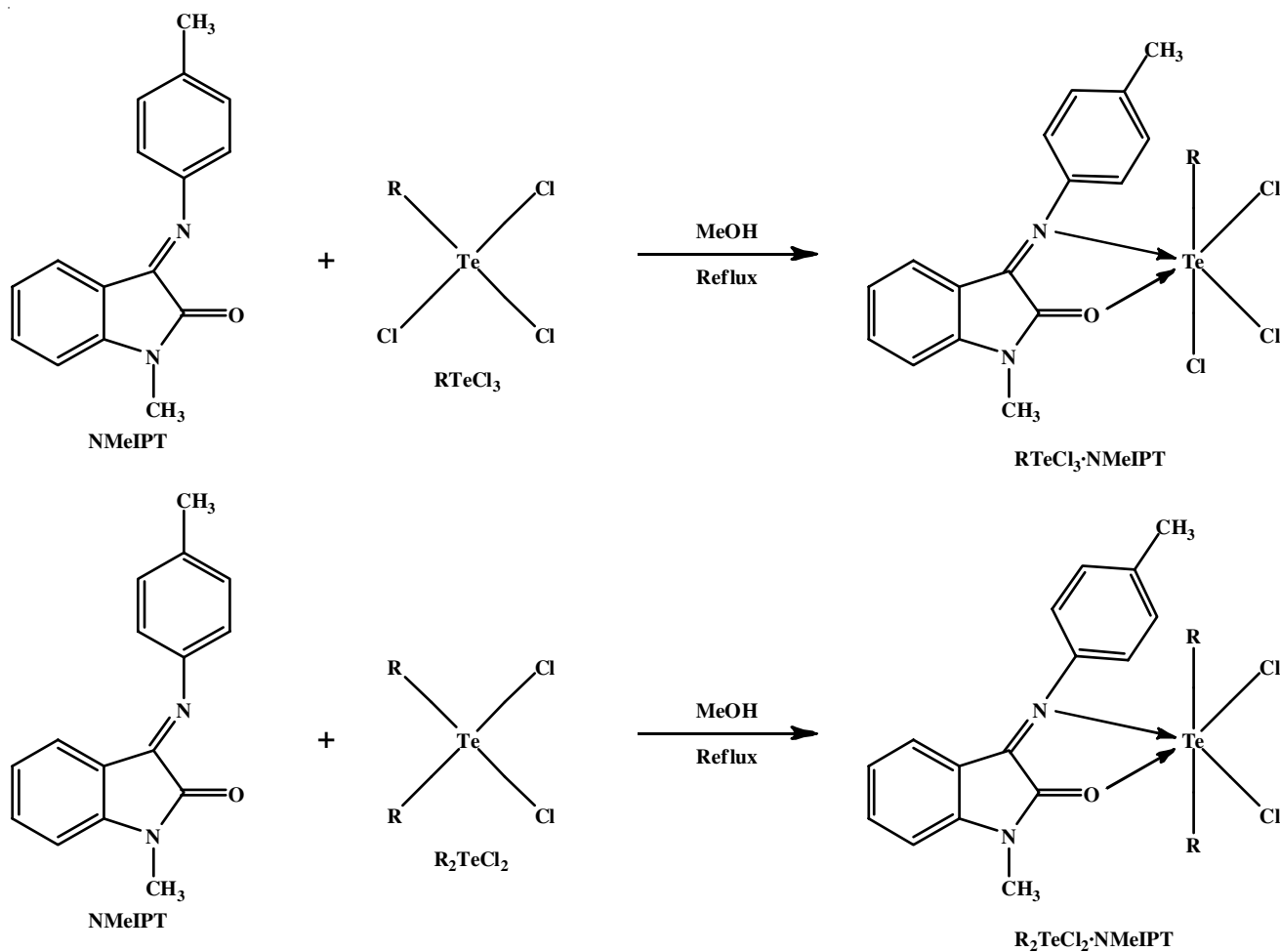


Scheme-I: Synthesis of NMeIPT (L)

philic substitution reaction of TeCl₄ with phenol, methoxybenzene and *o*-methylphenol in 1:1 and 1:2 molar ratio led to the formation of RTeCl₃ and R₂TeCl₂ as reported in the literature [25-30] (**Scheme-II**).



Synthesis of organotellurium(IV) complexes (RTeCl₃·NMeIPT and R₂TeCl₂·NMeIPT): All the organotellurium(IV) complexes were synthesized by addition of 20 mL methanolic solution of ligand NMeIPT (0.01 mol) mixed with 20 mL methanolic solutions of RTeCl₃/R₂TeCl₂ (0.01 mol) and refluxed



Scheme-II: Synthesis of RTeCl₃·NMeIPT and R₂TeCl₂·NMeIPT

for 4 h on a magnetic stirrer at 80 °C. Excessive solvent was distilled off and kept at room temperature for 3-4 days. The coloured complexes formed were recrystallized from methanol and dried in desiccator over anhydrous CaCl₂ (**Scheme-II**).

RTeCl₃·NMeIAP (4-hydroxyphenyl) (2a): *m.w.* 577.96 g/mol; *m.p.*: 132-134 °C; *yield*: 85.22%, colour: dark brown. ¹H NMR (600 MHz, DMSO-*d*₆, δ ppm): 10.62 (s, 1H, Ar-OH), 8.22-6.75 (m, 12H, Ar-H), 3.21 (s, 3H, N-CH₃), 2.42 (s, 3H, -CH₃). ¹³C NMR (600 MHz, DMSO-*d*₆, δ ppm): 183.34 (C₉), 157.53 (C₂), 155.92 (C₂₁), 151.85 (C₁₁), 142.24 (C₈), 138.66 (C₆), 134.73 (C₁₃, C₁₅), 130.51 (C₁₉, C₂₃), 129.74 (C₂₀, C₂₂), 121.62 (C₁₈), 124.71 (C₅), 123.65 (C₄), 123.57 (C₁₂, C₁₆), 117.86 (C₃), 116.92 (C₁₄), 111.04 (C₇), 26.49 (C₁₀), 20.42 (C₁₇). Elemental analysis for ligand **2a** (*m.f.*: C₂₂H₁₉N₂O₂TeCl₃) calcd. (found) %: C, 45.77 (45.54); H, 3.32 (2.96); N, 4.85 (4.84); Te, 22.10 (22.03); Cl, 18.42 (18.36).

RTeCl₃·NMeIAP (4-methoxyphenyl) (2b): *m.w.*: 591.98 g/mol; *m.p.*: 114-117 °C; *yield*: 87.61%, colour = black. ¹H NMR (600 MHz, DMSO-*d*₆, δ ppm): 8.32 – 6.54 (m, 12H, Ar-H), 3.21 (s, 3H, N-CH₃), 3.81 (s, 3H, OCH₃), 2.41 (s, 3H, -CH₃). ¹³C NMR (600 MHz, DMSO-*d*₆, δ ppm): 183.92 (C₉), 160.87 (C₂), 159.38 (C₂₀), 157.22 (C₂₁), 151.85 (C₁₁), 144.33 (C₈), 138.66 (C₆), 130.71 (C₁₉, C₂₃), 129.71 (C₁₃, C₁₅), 126.81 (C₁₂, C₁₆), 124.71 (C₅), 123.67 (C₄), 122.70 (C₁₅), 120.01 (C₁₈), 116.56 (C₂₀, C₂₂), 123.67 (C₄), 117.85 (C₃), 116.97 (C₁₄) 111.04 (C₇), 55.95 (C₂₃), 26.49 (C₁₀) 20.42 (C₁₇). Elemental analysis for ligand **2b** (*m.f.*: C₂₃H₂₁N₂O₂TeCl₃) calcd. (found) %: C, 46.71 (46.53); H, 3.58 (3.23); N, 4.74 (4.72); Te, 21.58 (21.50); Cl, 17.98 (17.92).

RTeCl₃·NMeIAP (3-methyl-4-hydroxyphenyl) (2c): *m.w.*: 591.97 g/mol; *m.p.*: 118-120 °C, *yield*: 75.39%, colour: yellow. ¹H NMR (600 MHz, DMSO-*d*₆, δ ppm): 10.14 (s, 1H, Ar-OH), 7.69 – 6.51 (m, 11H, Ar-H), 3.14 (s, 3H, N-CH₃), 2.19 (s, 3H, -CH₃), 2.41 (s, 3H, -CH₃). ¹³C NMR (600 MHz, DMSO-*d*₆, δ ppm): 183.94 (C₉), 158.66 (C₂), 157.52 (C₂₁), 151.85 (C₁₁), 141.70 (C₈), 138.66 (C₆), 134.72 (C₁₈), 133.99 (C₁₉), 133.36 (C₁₃, C₁₅), 130.51 (C₂₂), 125.60 (C₁₂, C₁₆), 124.71 (C₅), 123.87 (C₂₀), 123.67 (C₄), 123.24 (C₁₈), 122.70 (C₁₅), 121.26 (C₁₇), 119.99 (C₂₃), 117.85 (C₃), 116.60 (C₁₄), 114.24 (C₂₂), 111.04 (C₇), 16.71 (C₂₄), 26.49 (C₁₀), 20.42 (C₁₇). Elemental analysis for ligand **2c** (*m.f.*: C₂₃H₂₁N₂O₂TeCl₃) calcd. (found) %: C, 46.71 (46.94); H, 3.58 (3.82); N, 4.74 (3.97); Te, 21.58 (20.35); Cl, 17.98 (19.02).

R₂TeCl₂·NMeIAP (4-Hydroxyphenyl) (2d): *m.w.*: 636.03 g/mol; *m.p.*: 96-98 °C, *yield*: 82.98%, colour: dark brown. ¹H NMR (600 MHz, DMSO-*d*₆, δ ppm): 10.10 (s, 2H, Ar-OH), 8.06-6.48 (m, 16H, Ar-H), 3.21 (s, 3H, N-CH₃), 2.42 (s, 3H, -CH₃). ¹³C NMR (600 MHz, DMSO-*d*₆, δ ppm): 183.32 (C₉), 157.53 (C₂), 155.92 (C₂₁, C₂₇), 151.85 (C₁₁), 142.23 (C₈), 138.65 (C₆), 134.73 (C₁₃, C₁₅), 130.51 (C₁₉, C₂₃, C₂₅, C₂₉), 129.74 (C₂₀, C₂₂, C₂₆, C₂₈), 121.62 (C₁₈, C₂₄), 124.71 (C₅), 123.65 (C₄), 123.57 (C₁₂, C₁₆), 117.90 (C₃), 116.92 (C₁₄), 111.04 (C₇), 26.49 (C₁₀), 20.42 (C₁₇). Elemental analysis for ligand **2d** (*m.f.*: C₂₈H₂₄N₂O₃TeCl₂) calcd. (found) %: C, 52.96 (52.3); H, 3.81 (4.06); N, 4.41 (3.85); Te, 20.06 (19.52); Cl, 11.17 (11.75).

R₂TeCl₂·NMeIAP (4-methoxyphenyl) (2e): *m.w.* 663.06 g/mol; *m.p.*: 106-107 °C, *yield*: 86.15%, colour: reddish brown.

¹H NMR (600 MHz, DMSO-*d*₆, δ ppm): 8.34-6.76 (m, 16H, Ar-H), 3.14 (s, 3H, N-CH₃), 3.86 (s, 6H, OCH₃), 2.41 (s, 3H, -CH₃). ¹³C NMR (600 MHz, DMSO-*d*₆, δ ppm): 183.92 (C₉), 160.80 (C₂), 157.22 (C₂₁, C₂₈), 151.85 (C₁₁), 144.33 (C₈), 138.66 (C₆), 130.71 (C₁₉, C₂₃, C₂₆, C₃₀), 129.71 (C₁₃, C₁₅), 126.81 (C₁₂, C₁₆), 124.71 (C₅), 123.67 (C₄), 122.70 (C₁₅), 120.01 (C₁₈, C₂₅), 116.56 (C₂₀, C₂₂, C₂₇, C₂₉), 123.67 (C₄), 117.87 (C₃), 116.56 (C₁₄) 111.04 (C₇), 55.95 (C₂₄, C₃₁), 26.50 (C₁₀), 20.42 (C₁₇). Elemental analysis for ligand **2e** (*m.f.*: C₃₀H₂₈N₂O₃TeCl₂) calcd. (found) %: C, 54.34 (54.22); H, 4.27 (4.26); N, 4.23 (3.99); Te, 19.24 (18.34); Cl, 10.69 (11.26).

R₂TeCl₂·NMeIAP (3-methyl-4-hydroxyphenyl) (2f): *m.w.* 663.06 g/mol, *m.p.*: 98-100 °C, *yield*: 76.27%, colour: dark yellow. ¹H NMR (600 MHz, DMSO-*d*₆, δ ppm): 10.16 (s, 2H, Ar-OH), 7.68 – 6.51 (m, 14H, Ar-H), 3.21 (s, 3H, N-CH₃), 2.19 (s, 6H, -CH₃), 2.42 (s, 3H, -CH₃). ¹³C NMR (600 MHz, DMSO-*d*₆, δ ppm): 183.94 (C₉), 158.40 (C₂), 157.53 (C₂₁, C₂₈), 151.85 (C₁₁), 141.70 (C₈), 138.66 (C₆), 134.72 (C₁₈, C₂₅), 134.01 (C₁₉, C₂₃, C₂₆, C₃₀) 133.36 (C₁₃, C₁₅), 125.60 (C₁₂, C₁₆), 124.71 (C₅), 123.87 (C₂₀, C₂₇), 123.67 (C₄), 123.24 (C₁₈), 122.70 (C₁₅), 121.26 (C₁₇), 119.99 (C₂₃), 117.85 (C₃), 116.60 (C₁₄), 114.24 (C₂₂, C₂₉), 111.04 (C₇), 16.57 (C₂₄, C₃₁), 26.49 (C₁₀), 20.41 (C₁₇). Elemental analysis for ligand **2f** (*m.f.*: C₃₀H₂₈N₂O₃TeCl₂) calcd. (found) %: C, 54.34 (54.01); H, 4.26 (4.17); N, 4.23 (3.89); Te, 19.24 (17.96); Cl, 10.69 (11.85).

in vitro Antimicrobial activity: Kirby Bauer disc diffusion method was used to screen all the synthesized complexes against the bacterial species *Bacillus cereus* and *Xanthomonas campestris*. The ligand (NMeIPT) and organotellurium(IV) complexes were also screened against the fungal species *Candida albicans*, *Fusarium oxysporum* and *Sclerotinia sclerotium* cultured on potato dextrose agar medium and also performed by the disc diffusion method. Ciprofloxacin and erythromycin were used as the standard antimicrobial drugs in order to compare their activity. The nutrient agar medium was used to grow microorganisms. The discs were incubated at 37 °C and zone inhibition diameter was measured after 24 h for bacterial strains and 72 h for fungal strains. All the experiments were performed in triplicate to reduce error.

RESULTS AND DISCUSSION

All the synthesized organotellurium(IV) complexes are coloured solids and soluble in ethanol, methanol, DMSO and DMF. Molar (Λ_M) conductivity of all the organotellurium(IV) complexes (**2a-2f**) at about 10⁻³ M at 25 °C were measured in DMSO. Molar conductivity (Λ_M) data for the complexes are compiled in Table-1. Molar conductance (Λ_M) values lie in the range of 39.15-126.21 ohm⁻¹ cm² mol⁻¹ predicts the non-electrolytic to 1:1 weak electrolytic type behaviour probably due to the ionization into RTeCl₂·NMeIPT⁺/R₂TeCl·NMeIPT⁺ and Cl⁻ in DMSO. Due to steric aspects and donor nature of DMSO, some of these complexes show higher molar conductance values to results probably due to the dissociation into solvated cation and [NMeIPT]⁻ along with Cl⁻. Transition metal complexes are reported to be non-electrolytic [31-33], which is different from tellurium(IV) complexes of Schiff base.

TABLE-1
MOLAR CONDUCTANCE VALUES OF THE
SYNTHESIZED ORGANOTELLURIUM(IV) COMPLEXES

Compound	Molar conductance (Ohm ⁻¹ cm ² mol ⁻¹)
2a	97.94
2b	119.50
2c	96.82
2d	112.48
2e	126.21
2f	39.15

Mass spectra: Mass spectra of the ligand and its organotellurium(IV) complexes were recorded at an electronic energy of 70 eV. The mass spectrum [34] of Schiff base (NMeIPT) (Fig. 1) showed molecular ion peak at $m/z = 251$ (M^+) refers to the formula mass of the ligand (molar mass = 252 g mol⁻¹). The fragments peaks at $m/z = 222.14$ and 144.98 are due to loss of two methyl groups and phenyl group. The relative intensity explains the stability of the various fragments of ligand and its complexes. The mass spectra of different organotellurium(IV) complexes **2a**, **2b**, **2c**, **2d**, **2e**, **2f** show the molecular ion peak at $m/z = 578.16$, 591.28, 591.57, 636.81, 664.13 and 663.74 respectively, which is equivalent to molecular mass of the organotellurium(IV) complexes. The data suggests the (1:1) molar ratio of $R_2TeCl_3 \cdot NMeIPT$ and $R_2TeCl_2 \cdot NMeIPT$ complexes.

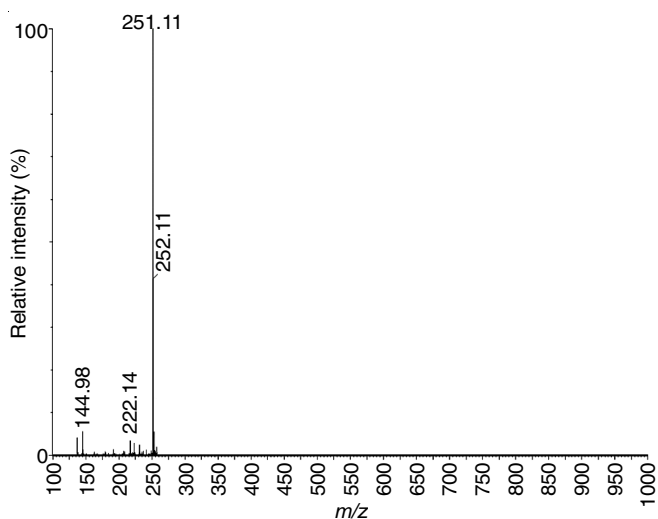


Fig. 1. Mass spectrum of the ligand NMeIPT

IR spectra: The results of FT-IR spectra of Schiff base ligand and organotellurium(IV) complexes are presented in Table-2. Comparison of different bands in the infrared spectra

TABLE-2
FT-IR FREQUENCIES (cm⁻¹) OF LIGAND (NMeIPT) AND ITS ORGANOTELLURIUM(IV) COMPLEXES

Compound	$\nu(C-H)$ aromatic stretching	$\nu(C-H)$ stretching	$\nu(C=O)$	$\nu(C=N)$	$\nu(Te-N)$	$\nu(Te-O)$
L	3063 m	2937 w	1736 s	1627 s	-	-
2a	3058 w	2922 w	1720 s	1611 s	289 m	501 m
2b	3060 w	2934 w	1721 s	1611 s	293 m	495 m
2c	3058 w	2936 w	1720 s	1610 s	290 m	503 m
2d	3059 w	2926 w	1721 s	1612 s	287 m	502 m
2e	3061 w	2936 w	1718 s	1611 s	292 m	498 m
2f	3058 w	2924 w	1709 s	1608 s	289 m	501 m

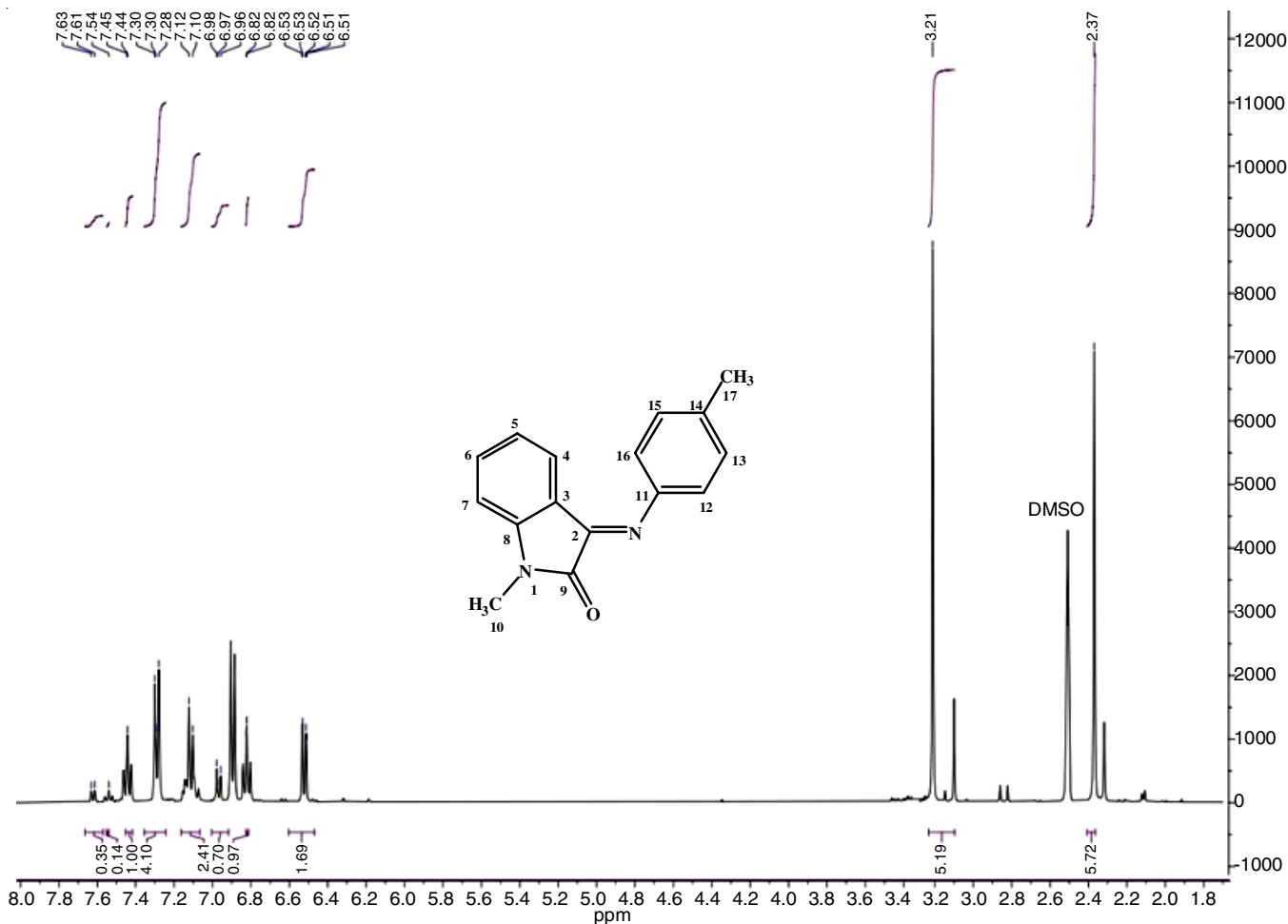
of ligand and organotellurium(IV) complexes determine the coordination sites from ligand to tellurium metal. The FT-IR spectrum of ligand showed different bands [23,35,36] at 3063, 1736 and 1627 cm⁻¹ assigned to $\nu(C-H)$, $\nu(C=O)$ and $\nu(C=N)$, respectively. The $\nu(C=O)$, band in all the complexes shifted to lower wavenumber in the region 1721-1709 cm⁻¹ indicating coordination of carbonyl oxygen to tellurium. In FT-IR spectra of all complexes, the characteristic azomethine [37] $\nu(C=N)$ band appears in the region 1611-1608 cm⁻¹ also showed shift to lower wavenumber indicates that nitrogen is coordinated to tellurium metal [24]. Further, appearance of two new bands in the 495-503 cm⁻¹ and 287-293 cm⁻¹ region in the spectra of the tellurium(IV) complexes are assigned due to Te-N and Te-O stretching frequency, respectively confirmed that azomethine nitrogen and carbonyl oxygen are involved in coordination [14,16,38].

¹H NMR spectra: ¹H NMR spectra of the ligand and all the organotellurium(IV) complexes were recorded in DMSO-*d*₆ and their spectral data are presented in Table-3. Singlet peak was observed at δ 3.21 ppm in the spectrum of all complexes which is due to N-CH₃ protons. The aromatic ring protons [39,40], in spectrum of Schiff base ligand are observed as multiplet in the region δ 6.51-7.63 ppm (Fig. 2). In ¹H NMR spectra of organotellurium(IV) complexes, aromatic protons slightly shift downfield and observed at δ 6.76-8.34 ppm. This may be due to the decrease of electron density after complexation, which supports the involvement of azomethine nitrogen and carbonyl oxygen atom in coordination with tellurium metal [24].

TABLE-3
¹H NMR SPECTRAL DATA OF THE LIGAND (NMeIPT)
AND ITS ORGANOTELLURIUM(IV) COMPLEXES

Compd.	Chemical shift (δ ppm (DMSO- <i>d</i> ₆))		
	Aromatic protons	N-CH ₃ protons	Methyl protons (<i>p</i> -toluidine ring)
L	7.63-6.51 (m, 8H)	3.21 (s, 3H)	2.37 (s, 3H)
2a	8.22-6.75 (m, 12H)	3.21 (s, 3H)	2.42 (s, 3H)
2b	8.32-6.54 (m, 12H)	3.21 (s, 3H)	2.41 (s, 3H)
2c	7.69-6.51 (m, 11H)	3.21 (s, 3H)	2.40 (s, 3H)
2d	8.06-6.48 (m, 16H)	3.21 (s, 3H)	2.42 (s, 3H)
2e	8.34-6.76 (m, 16H)	3.21 (s, 3H)	2.41 (s, 3H)
2f	7.68-6.51 (m, 14H)	3.21 (s, 3H)	2.42 (s, 3H)

¹³C NMR spectra: ¹³C NMR spectra of Schiff base and its organotellurium(IV) complexes were recorded in DMSO-*d*₆ and their spectral data are presented in Table-4. In the ¹³C

Fig. 2. ^1H NMR spectrum of ligand (NMeIPT)TABLE-4
 ^{13}C NMR SPECTRAL DATA OF THE LIGAND (NMeIPT) AND ORGANOTELLURIUM(IV) COMPLEXES

Compound	Chemical shift, δ ppm (DMSO- d_6)			
	C=O	CH	C=N	Aromatic carbons
L	162.84 (C ₉)	26.49 (C ₁₀), 20.42 (C ₁₇)	155.24 (C ₂)	147.80 (C ₁₁), 145.82 (C ₈), 138.09 (C ₆), 134.30 (C _{13, 15}), 122.10 (C ₁₅), 122.91 (C ₅), 119.97 (C ₄), 119.12 (C ₃), 116.90 (C ₁₄) 110.29 (C ₇), 126.28 (C _{12, 16}).
2a	183.34 (C ₉)	26.49 (C ₁₀), 20.42 (C ₁₇)	157.53 (C ₂)	155.92 (C ₂₁), 151.85 (C ₁₁), 142.24 (C ₈), 138.66 (C ₆), 134.73 (C _{13, 15}), 130.51 (C _{19, 23}), 129.74 (C _{20, 22}), 121.62 (C ₁₈), 124.71 (C ₅), 123.65 (C ₄), 123.57 (C _{12, 16}), 117.86 (C ₃), 116.92 (C ₁₄), 111.04 (C ₇).
2b	183.92 (C ₉)	55.95 (C ₂₄), 26.49 (C ₁₀), 20.42 (C ₁₇)	160.87 (C ₂)	157.22 (C ₂₁), 151.85 (C ₁₁), 144.33 (C ₈), 138.66 (C ₆), 130.71 (C _{19, 23}), 129.71 (C _{13, 15}), 126.81 (C _{12, 16}), 124.71 (C ₅), 123.67 (C ₄), 122.70 (C ₁₅), 120.01 (C ₁₈), 116.56 (C _{20, 22}), 123.67 (C ₄), 117.85 (C ₃), 116.97 (C ₁₄) 111.04 (C ₇).
2c	183.94 (C ₉)	16.71 (C ₂₄), 26.49 (C ₁₀), 20.42 (C ₁₇)	158.66 (C ₂)	157.52 (C ₂₁), 151.85 (C ₁₁), 141.70 (C ₈), 138.66 (C ₆), 134.72 (C ₁₈), 133.99 (C ₁₉), 133.36 (C _{13, 15}), 130.51 (C ₂₂), 125.60 (C _{12, 16}), 124.71 (C ₅), 123.87 (C ₂₀), 123.67 (C ₄), 123.24 (C ₁₈), 122.70 (C ₁₅), 121.26 (C ₁₇), 119.99 (C ₂₃), 117.85 (C ₃), 116.60 (C ₁₄), 114.24 (C ₂₂), 111.04 (C ₇).
2d	183.32 (C ₉)	26.49 (C ₁₀), 20.42 (C ₁₇)	157.53 (C ₂)	155.92 (C _{21, 27}), 151.85 (C ₁₁), 142.23 (C ₈), 138.65 (C ₆), 134.73 (C _{13, 15}), 130.51 (C _{19, 23}), 129.74 (C _{20, 22, 26, 28}), 121.62 (C _{18, 24}), 124.71 (C ₅), 123.65 (C ₄), 123.57 (C _{12, 16}), 117.90 (C ₃), 116.92 (C ₁₄), 111.04 (C ₇).
2e	183.92 (C ₉)	55.95 (C _{24, 31}), 26.50 (C ₁₀)	160.80 (C ₂)	157.22 (C _{21, 28}), 151.85 (C ₁₁), 144.33 (C ₈), 138.66 (C ₆), 130.71 (C _{19, 23, 26, 30}), 129.71 (C _{13, 15}), 126.81 (C _{12, 16}), 124.71 (C ₅), 123.67 (C ₄), 122.70 (C ₁₅), 120.01 (C _{18, 25}), 116.56 (C _{20, 22, 27, 29}), 123.67 (C ₄), 117.87 (C ₃), 116.56 (C ₁₄) 111.04 (C ₇).
2f	183.94 (C ₉)	16.57 (C _{24, 31}), 26.49 (C ₁₀)	158.40 (C ₂)	157.53 (C _{21, 28}), 151.85 (C ₁₁), 141.70 (C ₈), 138.66 (C ₆), 134.72 (C _{18, 25}), 134.01 (C _{19, 23}), 133.36 (C _{13, 15}), 125.60 (C _{12, 16}), 124.71 (C ₅), 123.87 (C _{20, 27}), 123.67 (C ₄), 123.24 (C ₁₈), 122.70 (C ₁₅), 121.26 (C ₁₇), 119.99 (C ₂₃), 117.85 (C ₃), 116.60 (C ₁₄), 114.24 (C _{22, 29}), 111.04 (C ₇).

NMR spectrum of Schiff base (NMeIPT), the carbon atom attached to carbonyl oxygen (C-9) and azomethine nitrogen (C-2) are observed at δ 160.79 and 157.22 ppm, respectively, which shift toward downfield frequency [7] in all studied organotellurium(IV) complexes and resonate at δ 183.92 and 157.53-160.87 ppm, respectively indicating coordination of ligand to tellurium metal *via* nitrogen and oxygen atom. The resonating values of aromatic carbons [41] of the ligand as well as complexes are given in the experimental section.

UV-vis spectra: The UV-vis spectral data of the ligand and its organotellurium(IV) complexes in solid state are reported in Table-5. The UV-visible spectrum of Schiff base ligand (NMeIPT) showed different bands [42,43] observed at 222, 288 and 442 nm. A band observed at 218 nm is attributed to (π - π^*) transition of isatin moiety and aromatic phenyl group of the ligand. On complexation, this band showed bathochromic shift and observed at 240 ± 2 nm (Fig. 3). Similarly, azomethine group ($-\text{C}=\text{N}-$) absorbs at 288 nm attributed to (n - π^*) transition, shifts to a longer wavelength and absorbs in the region 303-314 nm in case of complexes. Further, a band in the spectrum of the Schiff base at 442 nm can be assigned to a charge transfer band within the *N*-methylisatin moiety. The shift towards longer wavelength in the organotellurium(IV) complexes indicating the coordination of azomethine nitrogen and oxygen atoms [23] to the tellurium metal.

TABLE-5
UV-VIS SPECTRAL DATA OF THE LIGAND (NMeIPT)
AND ITS ORGANOTELLURIUM(IV) COMPLEXES

Compd.	λ_{max} (π - π^*) (nm)	λ_{max} (n - π^*) (nm)	λ_{max} (CT) (nm)
L	222	288	442
2a	240	305	463
2b	241	312	462
2c	238	314	461
2d	241	306	463
2e	238	313	461
2f	239	303	462

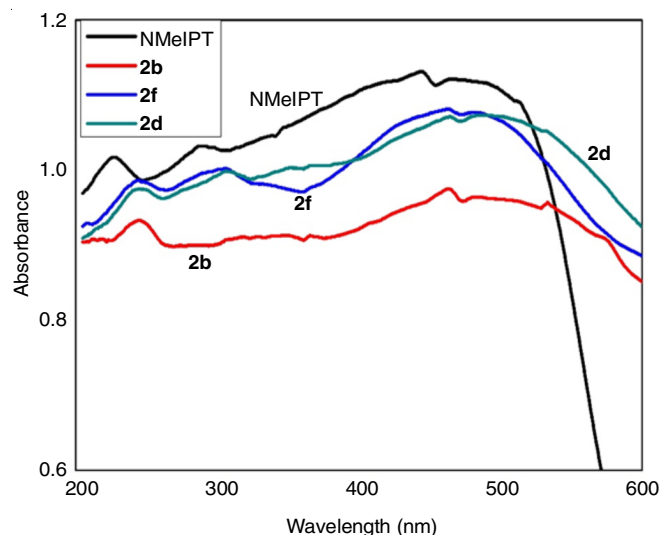


Fig. 3. UV-Vis spectra of the NMeIPT, 2b, 2d and 2f

Molecular modelling: The 3D geometry of the Schiff base (NMeIPT) and its organotellurium(IV) complexes (2a and 2e) are optimized and DFT calculations was carried out by using Orca Visualization program with Avogadro 4.0 version. Fully optimized molecular structure of ligand and organotellurium complexes (2a and 2e) are shown in Fig. 4 and their bond lengths are compared and listed in Table-6. Bond angle and bond length values surrounding the tellurium metal are characteristic of distorted octahedral geometry of the complexes, which is in agreement with the proposed structures. In ligand, the azomethine C=N and C=O bond lengths are 1.312 Å and 1.212 Å, respectively. In complexes, these C=N bond length become slightly shorter and C=O bond length become longer. This variation indicates the coordination of azomethine and carbonyl group *via* N and O atoms. Selected bond lengths of complex 2a are Te- azomethine-N (2.072 Å), Te-carbonyl-O (1.992 Å), Te-phenolic-C (2.137 Å) and three Te-Cl (2.41Å) complete the distorted coordination sphere of metal.

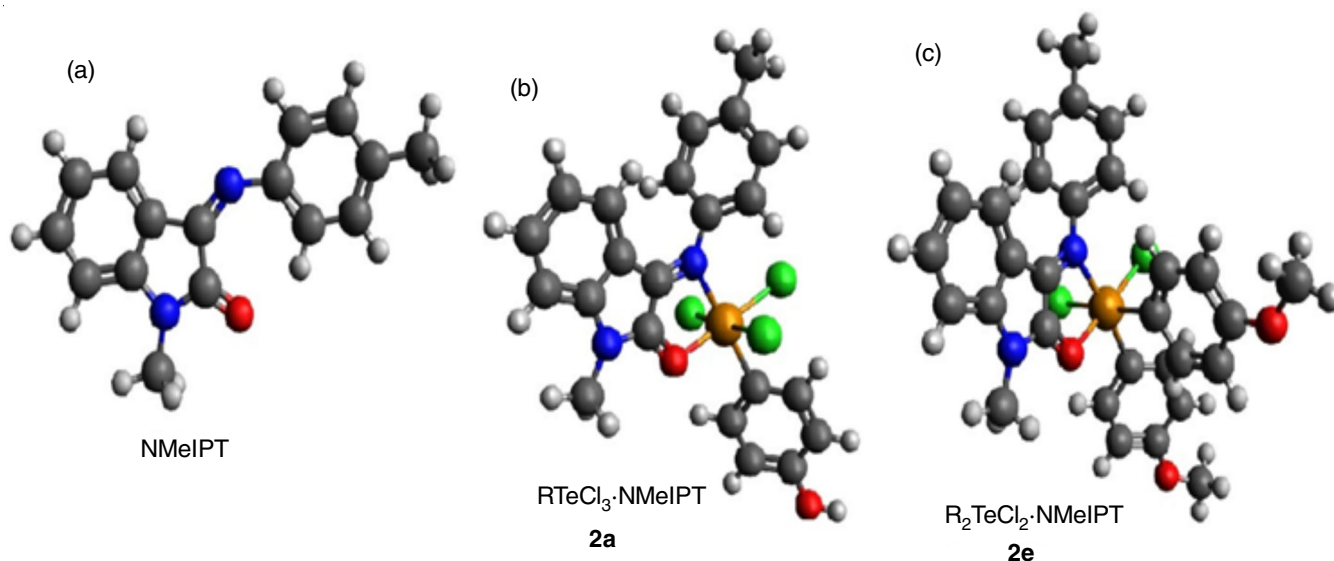


Fig. 4. (a) Optimized structure of NMeIPT (b) Optimized structure of 2a (c) Optimized structure of 2e. Color code: blue-N; red-O; grey-C; white-H; green- Cl; yellow-Te

Compd.	C=N	C=O	Te-N (azomethine)	Te-O (carbonyl)
L	1.312	1.212	-	-
2a	1.295	1.223	2.072	1.992
2e	1.298	1.221	2.084	1.987

DFT study: HOMO (highest occupied molecular orbital) and LUMO (lowest unoccupied molecular orbital) are the key molecular orbitals which are responsible for chemical stability of the molecule. HOMO and LUMO for ligand and its organo-tellurium(IV) complexes (**2a** and **2e**) are obtained from DFT calculations (def2-SVP) using Avogadro 4.0 with ORCA program. The HOMO-LUMO energy gap (ΔE) is an important stability index, for ligand its value found to be 4.208 eV whereas for complexes **2a** and **2e**, the energy gap reasonably reduced [44] to 3.960 and 3.982 eV, respectively due to establishment of coordination band between ligand and tellurium metal. The smaller energy gap for complexes explains the stability. Quantum chemical parameters [45,46] of the compounds such as electronegativity (χ), softness (S), hardness (η), electrophilicity index (ω) and chemical potential (Π) are obtained from calculations such as energies of HOMO and LUMO (Table-7). In ligand, HOMO and LUMO is spread over whole π -moiety. HOMO is spread over whole π -moiety of ligand with less contribution of tellurium metal and LUMO is spread over the surrounding of tellurium metal in complexes (Fig. 5).

in vitro Antimicrobial activity: Antimicrobial activity of the Schiff base (NMeIPT) and its tellurium(IV) complexes

Parameters	Ligand	2a	2e
E_{HOMO} (eV)	-7.212	-4.093	-4.096
E_{LUMO} (eV)	-3.004	-0.133	-0.114
ΔE (eV)	4.208	3.960	3.982
IE (eV)	7.212	4.093	4.096
χ (eV)	5.108	2.113	2.105
η (eV)	2.104	1.980	1.991
S (eV) ⁻¹	0.2376	0.2525	0.2511
ω (eV)	6.199	1.1273	1.1126
Π	-5.108	-2.113	-2.105

have been carried out against bacterial strains (*Bacillus cereus*, *Xanthomonas campestris*) and fungal strains (*Fusarium oxysporum*, *Candida albicans*, *Sclerotinia sclerotium*). Zone of inhibition in cm for the ligand and complexes are listed in Table-8. The results showed that Schiff base ligand has moderate activity in the antibacterial species while showed better activity against antifungal species. The observation indicates that the tellurium(IV) complexes are more active than free Schiff base ligand due to chelation, can be explained by Overtone's idea and chelation theory. Organotellurium(IV) complexes **2a** and **2e** showed good antibacterial activity against *Bacillus cereus* and **2a** and **2d** possess better antibacterial activity against *Xanthomonas campestris*. Complex **2a** is the most active against all fungi. All compounds show less antifungal activity towards *Fusarium oxysporum* and *Sclerotinia sclerotium* but good activity against *Candida albicans* as compared to the standard

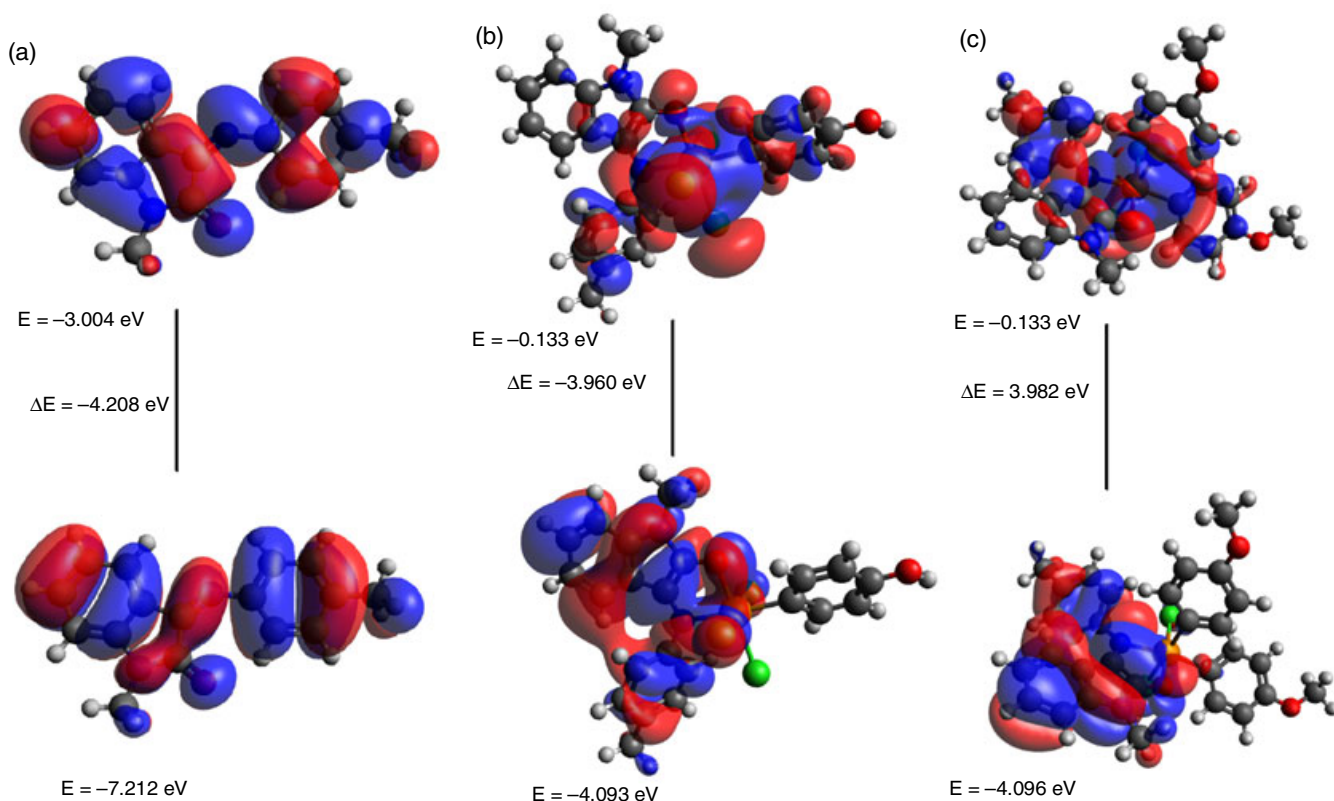


Fig. 5. (a) HOMO and LUMO with energy gap of NMeIPT (b) HOMO and LUMO with energy gap of **2a** (c) HOMO and LUMO with energy gap of **2e**

TABLE-8
ZONE INHIBITION DIAMETER (cm) OF LIGAND (NMeIPT) AND ITS ORGANOTELLURIUM(IV) COMPLEXES

Compound	Antibacterial activity (diameter in cm)		Antifungal activity (diameter in cm)		
	<i>Bacillus cereus</i>	<i>Xanthomonas campestris</i>	<i>Fusarium oxysporum</i>	<i>Candida albicans</i>	<i>Sclerotinia sclerotium</i>
L	0.2	0.3	1.3	1.8	1.4
2a	1.4	1.4	1.5	2.0	1.6
2b	1.2	0.8	1.3	1.8	1.0
2c	1.0	0.8	1.2	1.2	1.2
2d	0.8	1.2	1.0	1.5	0.7
2e	1.3	0.9	1.4	1.7	0.9
2f	0.9	0.5	1.3	1.4	1.1
Ciprofloxacin	1.4	1.2	–	–	–
Erythromycin	–	–	1.6	1.8	1.8

drug (*erythromycin*). Complex **2a** is the most active among all complexes showing considerable results against all fungi. Thus, tellurium complexes are more biologically active than Schiff base and act as hopeful antimicrobial drug contenders.

Conclusion

New organotellurium(IV) complexes (**2a-f**) of Schiff base ligand were synthesized and characterized by conductance measurement, mass spectrometry, elemental analyses, FT-IR, mass, ^1H & ^{13}C NMR and UV-vis spectral studies. The various spectroscopic techniques suggest the distorted octahedral geometry for all the synthesized organotellurium(IV) complexes ($\text{R}_2\text{TeCl}_3\text{-NMeIPT}$ and $\text{R}_2\text{TeCl}_2\text{-NMeIPT}$) and Schiff base (NMeIPT) acts as a bidentate O-(carbonyl) and *N*-(azomethine linkage) chelating ligand. Molecular modelling has been used to optimize the geometry of Schiff base (NMeIPT) and its metal complexes. The antimicrobial activity of the ligand and its organotellurium(IV) complexes against bacterial and fungal strains have been evaluated. The study shows that complexes show more biological activity than standard drugs.

ACKNOWLEDGEMENTS

The authors are thankful to Maharishi Dayanand University, Rohtak, India for providing the necessary research facilities. One of the authors, (MK) is also thankful to UGC, New Delhi, India for providing the Senior Research Fellowship. Thanks are also due to IIT Ropar, for conducting the mass analyses, SAIF, Punjab University for CHN analyses, G.J. University, Hisar for NMR studies and CCS Haryana Agricultural University, Hissar, India for the antimicrobial activities.

CONFLICT OF INTEREST

The authors declare that there is no conflict of interests regarding the publication of this article.

REFERENCES

1. B. Iftikhar, K. Javed, M.S.U. Khan, Z. Akhter, B. Mirza and V. Mckee, *J. Mol. Struct.*, **1155**, 337 (2018); <https://doi.org/10.1016/j.molstruc.2017.11.022>
2. W.H. Mahmoud, R.G. Deghadi and G.G. Mohamed, *Appl. Organomet. Chem.*, **30**, 221 (2016); <https://doi.org/10.1002/aoc.3420>
3. S.N. Pandeya, D. Sriram, G. Nath and E. De Clercq, *Arzneimittel-Forschung Drug Res.*, **50**, 55 (2000); <https://doi.org/10.1055/s-0031-1300164>
4. S.N. Pandeya, D. Sriram, G. Nath and E. De Clercq, *Eur. J. Med. Chem.*, **35**, 249 (2000); [https://doi.org/10.1016/S0223-5234\(00\)00125-2](https://doi.org/10.1016/S0223-5234(00)00125-2)
5. S.P. Chavan and R. Sivappa, *Tetrahedron Lett.*, **45**, 3941 (2004); <https://doi.org/10.1016/j.tetlet.2004.03.089>
6. K.S. Kumar, S. Ganguly, R. Veerasamy and E. De Clercq, *Eur. J. Med. Chem.*, **45**, 5474 (2010); <https://doi.org/10.1016/j.ejmech.2010.07.058>
7. S. Smitha, S.N. Pandeya, J.P. Stables and S. Ganapathy, *Sci. Pharm.*, **76**, 621 (2008); <https://doi.org/10.3797/scipharm.0806-14>
8. A. Kajal, S. Bala, S. Kamboj, N. Sharma and V. Saini, *J. Catal.*, **2013**, 893512 (2013); <https://doi.org/10.1155/2013/893512>
9. G. Kumar, D. Kumar, C.P. Singh, A. Kumar and V.B. Rana, *J. Serb. Chem. Soc.*, **75**, 629 (2010); <https://doi.org/10.2298/JSC090704037K>
10. C.M. Da Silva, D.L. Da Silva, L.V. Modolo, R.B. Alves, M.A. De Resende, C.V.B. Martins and Á. De Fátima, *J. Adv. Res.*, **2**, 1 (2011); <https://doi.org/10.1016/j.jare.2010.05.004>
11. S.N. Pandeya, D. Sriram, G. Nath and E. De Clercq, *Farmaco*, **54**, 624 (1999); [https://doi.org/10.1016/S0014-827X\(99\)00075-0](https://doi.org/10.1016/S0014-827X(99)00075-0)
12. A.A. Bekhit, H.T.Y. Fahmy, S.A.F. Rostom and A.M. Baraka, *Eur. J. Med. Chem.*, **38**, 27 (2003); [https://doi.org/10.1016/S0223-5234\(02\)00009-0](https://doi.org/10.1016/S0223-5234(02)00009-0)
13. G. Goyat, S. Garg and K.K. Verma, *Chem. Sci. Trans.*, **5**, 479 (2016); <https://doi.org/10.7598/cst2016.1204>
14. Deepak, S. Chauhan, K.K. Verma and S. Garg, *Chem. Sci. Trans.*, **6**, 448 (2017); <https://doi.org/10.7598/cst2017.1394>
15. G. Goyat, A. Malik, S. Garg and K.K. Verma, *J. Chem. Pharm. Res.*, **8**, 218 (2016).
16. Deepak, S. Chauhan, K.K. Verma and S. Garg, *Chem. Sci. Trans.*, **6**, 339 (2017); <https://doi.org/10.7598/cst2017.1391>
17. S. Chauhan, Deepak, S. Garg and K.K. Verma, *Int. J. Chem. Sci.*, **14**, 269 (2016).
18. W.M.I. Hassan, E.M. Zayed, A.K. Elkholly G.G. Mohamed and H. Moustafa, *Spectrochimica Acta A Mol. Biomol. Spectrosc.*, **103**, 378 (2013); <https://doi.org/10.1016/j.saa.2012.10.058>
19. P. Rathi and D.P. Singh, *J. Mol. Struct.*, **1100**, 208 (2015); <https://doi.org/10.1016/j.molstruc.2015.07.025>
20. S. Gautam, S. Chandra, H. Rajor, S. Agrawal and P.K. Tomar, *Appl. Organomet. Chem.*, **32**, e3915 (2018); <https://doi.org/10.1002/aoc.3915>
21. A.I. Vogel, Practical Organic Chemistry, Including Qualitative Organic Analysis, Longmans, Green and Co.: London, New York, Toronto, Ed.: 3, vol. 1188, p. 300 (1956).
22. A. Weissberger, Technique of Organic Chemistry, Interscience Publishers, Inc.: New York, vol. 7 (1955).
23. A. Kriza and C. Parnau, *Acta Chim. Slov.*, **48**, 445 (2001).
24. G. Goyat, S. Garg and K.K. Verma, *Res. J. Pharm. Biol. Chem. Sci.*, **7**, 869 (2016).

25. G.T. Morgan and H.D.K. Drew, *J. Chem. Soc. Trans.*, **127**, 2307 (1925); <https://doi.org/10.1039/CT9252702307>
26. J. Bergman, *Tetrahedron*, **28**, 3323 (1972); [https://doi.org/10.1016/S0040-4020\(01\)93674-9](https://doi.org/10.1016/S0040-4020(01)93674-9)
27. N. Petragnani and H.A. Stefani, *Org. Synth.*, **1**, 9 (2007).
28. F.J. Berry, E.H. Kustan, M. Roshani and B.C. Smith, *J. Organomet. Chem.*, **99**, 115 (1975); [https://doi.org/10.1016/S0022-328X\(00\)86367-6](https://doi.org/10.1016/S0022-328X(00)86367-6)
29. B.L. Khandelwal, K. Kumar and K. Reina, *Synth. React. Inorg. Met. Chem.*, **11**, 65 (1981); <https://doi.org/10.1080/00945718108059276>
30. B.L. Khandelwal, K. Kumar and F.J. Berry, *Inorg. Chim. Acta*, **47**, 135 (1981); [https://doi.org/10.1016/S0020-1693\(00\)89319-6](https://doi.org/10.1016/S0020-1693(00)89319-6)
31. N.N. Greenwood, B.P. Straughan and A.E. Wilson, *J. Chem. Soc. A Inorg. Phys. Ther.*, **4**, 2209 (1968); <https://doi.org/10.1039/j19680002209>
32. W.J. Geary, *Coord. Chem. Rev.*, **7**, 81 (1971); [https://doi.org/10.1016/S0010-8545\(00\)80009-0](https://doi.org/10.1016/S0010-8545(00)80009-0)
33. A. Apelblat, *J. Solution Chem.*, **40**, 1234 (2011); <https://doi.org/10.1007/s10953-011-9718-y>
34. A.K. El-Sawaf, F. El-Essawy, A.A. Nassar and E.S.A. El-Samanody, *J. Mol. Struct.*, **1157**, 381 (2018); <https://doi.org/10.1016/j.molstruc.2017.12.075>
35. A.A. Abdel Aziz, I.S.A. El-Sayed and M.M.H. Khalil, *Appl. Organomet. Chem.*, **31**, e3730 (2017); <https://doi.org/10.1002/aoc.3730>
36. A.M.A. Hassaan and M.A. Khalifa, *Monatsh. Chem.*, **124**, 803 (1993); <https://doi.org/10.1007/BF00816402>
37. J.E. Kovacic, *Spectrochim. Acta A*, **23**, 183 (1967); [https://doi.org/10.1016/0584-8539\(67\)80219-8](https://doi.org/10.1016/0584-8539(67)80219-8)
38. Deepak, S. Chauhan, K.K. Verma and S. Garg, *Int. J. Chem. Sci.*, **15**, 182 (2017).
39. G. Goyat, A. Malik, S. Garg and K.K. Verma, *Int. J. Chem. Sci.*, **14**, 1498 (2016).
40. M. Verma, S.N. Pandeya, K.N. Singh and J.P. Stables, *Acta Pharm.*, **54**, 49 (2004).
41. M.C. Rodríguez-Argüelles, S. Mosquera-Vázquez, P. Tourón-Touceda, J. Sanmartín-Matalobos, A.M. García-Deibe, M. Belicchi-Ferrari, G. Pelosi, C. Pelizzi and F. Zani, *J. Inorg. Biochem.*, **101**, 138 (2007); <https://doi.org/10.1016/j.jinorgbio.2006.09.004>
42. R.M. Issa, A.M. Khedr and H.F. Rizk, *Spectrochim. Acta A Mol. Biomol. Spectrosc.*, **62**, 621 (2005); <https://doi.org/10.1016/j.saa.2005.01.026>
43. V.V. Raju, K.P. Balasubramanian, C. Jayabalakrishnan and V. Chinnusamy, *Nat. Sci.*, **3**, 542 (2011).
44. V.R. Chandrasekhar, K.M. Palsamy, R. Lokesh, D. Thangadurai T., I. Gandhi N., R. Jegathalaprathaban and R. Gurusamy, *Appl. Organomet. Chem.*, **33**, e4753 (2018); <https://doi.org/10.1002/aoc.4753>
45. T. Abbaz, A. Bendjeddou and D. Villemin, *Int. J. Adv. Sci. Eng. Technol.*, **5**, 5150 (2018).
46. A.Z. El-Sonbati, M.A. Diab, G.G. Mohamed, M.A. Saad, S.M. Morgan and S.E.A. El-Sawy, *Appl. Organomet. Chem.*, **33**, 1 (2019); <https://doi.org/10.1002/aoc.4973>